

## The relation between the northern polar cap and auroral electrojet geomagnetic indices in the wintertime

D. Vassiliadis<sup>1</sup>, V. Angelopoulos<sup>2</sup>, D. N. Baker<sup>3</sup>, A. J. Klimas<sup>4</sup>

**Abstract.** The polar cap (*PC*) index is a measure of the high-latitude geomagnetic disturbances due to Hall and field-aligned currents. The index is well correlated with the auroral electrojet *AL* and *AU* indices (correlation with the *PC* index is 76% and 66%, resp.). Here we obtain several types of data-based models that relate the *PC* to the *AL* and *AU* indices in the wintertime, when the ionospheric conductivity is mostly due to the precipitating particles of the field-aligned currents. The new models predict *AL* and *AU* from *PC* with correlations much higher than those found by earlier studies. Thus linear moving-average filters reproduce the observed *AL* with a correlation of 88% (*AU*: 75%) while linear autoregressive moving-average (ARMA) models based on the *PC* index produce in-sample single-step predictions with 98% and 97% correlations with *AL* and *AU* respectively. For long-term, out-of-sample prediction, the linear ARMA prediction from the *PC* index has an asymptotic prediction error which is at least 25% more accurate than the prediction from solar wind input. Nonlinear models are slightly more accurate than their linear counterparts, indicating a weak nonlinearity in the relation between the polar cap and auroral zone indices. The prediction-observation correlations are sufficiently high that models based on the *PC* index can be used for specification of the auroral geomagnetic activity.

### Polar Cap and Auroral Zone Geomagnetic Indices

The Polar Cap (*PC*) index measures geomagnetic disturbances at the polar cap which are due to ionospheric and field-aligned currents [Troshichev, 1988; Vennerstroem et al., 1991]. The former ones are Hall currents induced by field line convection and form a part of the DP2 current system. The relative importance of each current type depends on the ionospheric conductivity which is modulated on the dayside by the seasonally and daily varying solar illumination and on the nightside by particle precipitation.

The index is derived from the horizontal geomagnetic disturbance HDP2 at a standard high-latitude station which for the northern polar cap is Thule at 83.3° N (a separate index is calculated for the southern cap). The *PC* index was designed to measure the part of the HDP2 disturbance due to magnetospheric field line convection. Convection is assumed to be linearly correlated with the solar wind input and hence the

*PC* index is the part of HDP2 disturbance correlated with the solar wind input and normalized to its units (mV/m). The relation between the *PC* index and solar wind input varies as a function of season and UT [Troshichev, 1988; Vennerstroem et al., 1991].

The second source for polar cap geomagnetic disturbances are field aligned currents which become dominant in the wintertime, when the polar cap is dark and convection-induced currents wane significantly. At that time the *PC* index becomes well-correlated with the *AU* and *AL* indices. The indices measure the geomagnetic effects of the auroral electrojets, which connect the footpoints of field-aligned currents in the ionosphere [Mayaud, 1980; Holzer and Slavin, 1981; Akasofu et al., 1983; Baumjohann, 1986; Kroehl, 1989]. In winter (November-February) the correlations with *AL* vary with UT in the range 85–90% and with *AU* 60–70% while in summer (May-August) the *PC-AL* correlation drops (75–85%) and that of *PC-AU* increases (60–85%) [Troshichev et al., 1988; Vennerstroem et al., 1991]. Intermediate correlations occur during the equinox periods. Geomagnetic disturbances due to other current types, for example the DPY current, have a negligible correlation with the *PC* index [Vennerstroem et al., 1991].

In the following sections, linear and nonlinear data-based models use the three indices as independent magnetospheric variables, and significantly improve the above correlations making possible the specification of the electrojet indices from the polar cap index.

The database of *PC<sub>Thule</sub>* is from November 1, 1978, to February 28, 1979. The 1-min *AL/AU* indices, the 15-min *PC* index, and the 5 min ISEE-3-measured solar wind input, are linearly interpolated to a time resolution of 2.5 min so that there are  $N = 69,120$  points for each geomagnetic variable. Since the original *PC* data have 15 min resolution, the interpolated index does not contain information about higher-frequency disturbances; however such disturbances are associated with length scales short compared to the polar cap and can be omitted (O. Troshichev, V. Papitashvili, priv. comm., 1995).

### Regressions and Linear Moving-Average Filters

The correlation coefficient between *PC* and *AL* time series is 76% for the first 8192 points (Fig. 1a) (compared to 75–85% if the data are separated according to UT [Vennerstroem et al., 1991]). The correlation is maximized (77%) when *PC* is shifted in time to precede *AL* by 7.5 min, but in individual events each index may precede the other by more than 10 minutes. The *PC-AU* correlation is 66% (55–70% for individual UT [Vennerstroem et al., 1991]) and the correlation is maximum (69%) when *PC* is shifted by 17.5 min. (The maximum *AL-AU* correlation occurs when *AL* leads by 10 min.) Thus a typical disturbance begins at polar latitudes

<sup>1</sup>Universities Space Research Association, Greenbelt, Maryland.

<sup>2</sup>Space Science Laboratory, University of California, Berkeley.

<sup>3</sup>Laboratory for Atmospheric and Space Physics, University of Colorado, Boulder.

<sup>4</sup>Laboratory for Extraterrestrial Physics, NASA Goddard Space Flight Center, Greenbelt, Maryland.

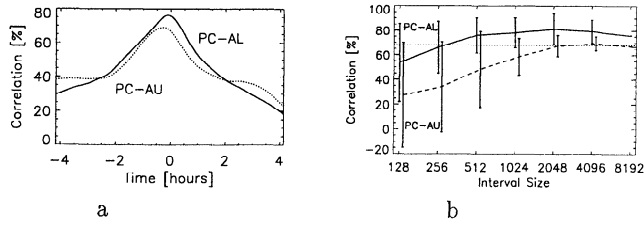


Figure 1. (a) Cross-correlation between  $PC$  and  $AL/AU$  indices. On the average, the  $PC$  index precedes  $AL$  by 7.5 min and  $AU$  by 17.5 min. (b) The correlation is calculated first over an interval of 8192 points and then over its subdivisions of lengths equal to powers of two. The variance of correlation values for each interval size is indicated by an error bar. The correlation increases with the interval size and asymptotes at approximately 80% for  $AL$  and 70% for  $AU$ .

on the nightside and then spreads equatorward reaching the auroral zone stations in several minutes [Rostoker and Phan, 1986]. Even when  $AU$  starts increasing before  $PC$ , the  $PC$  index reaches its maximum level faster. We examined the relative phase delay versus  $AL$  activity level, which might show a relation between rate of polar cap expansion and driven and loading-unloading effects, but we did not find a systematic dependence.

The  $PC$ - $AL$  correlation remains high (>70%) even for intervals as short as 10 hours (Fig. 1b, solid line). In contrast to that, high  $PC$ - $AU$  correlations occur only for intervals longer than 3.5 days (dotted line).

The high correlation coefficient is explained by a common cause for  $PC$  and  $AL/AU$ , i.e. field-aligned currents, or a causal relation between them. A regression of the electrojet indices on  $PC$  gives

$$\begin{aligned}\widehat{AL}_t &= -80.4 \cdot PC_{t-3} - 14.3 [nT] \\ \widehat{AU}_t &= 33.1 \cdot PC_{t-7} + 34.1 [nT]\end{aligned}\quad (1)$$

where the subscripts denote time measured in 2.5-min units, and the hat,  $\widehat{AL}$ , denotes either predicted or reproduced  $AL$ .

By including several previous  $PC$  values in the regression, we form a linear moving-average (MA) filter. For example for  $AL$  we have:

$$\widehat{AL}_{t+1} = \sum_{i=0}^{T-1} H_i PC_{t-i}, \quad (2)$$

We solve Eq. (2) numerically for the impulse response  $H$ , and convolve  $H$  with the  $PC$  data to get  $\widehat{AL}$ . The number of lags,  $T$ , is selected empirically so as to minimize the rms difference between observed and reproduced  $AL$ . For the first 5,000 points of our database the MA filter ( $T = 20$  min) reproduces  $AL_{t+1}$  to a moderate extent: the correlation between observation and in-sample prediction is 88% and the rms error is  $0.47 \sigma_{AL} = 58$  nT ( $\sigma_{AL}$  is the standard deviation of the 5,000  $AL$  data). The  $PC$ - $AU$  relation is weaker with an MA filter reproducing  $AU$  at a correlation of 75% and an rms error of  $0.66 \sigma_{AU} = 34$  nT.

## Linear Autoregressive Moving-Average Models

A linear regression on past  $PC$  and  $AL$  is a linear autoregressive moving-average (ARMA) model

$$\widehat{AL}_{t+1} = \sum_{i=0}^{m-1} A_i AL_{t-i} + \sum_{j=0}^{m-1} B_j PC_{t-j} \quad (3)$$

The high correlation between  $AL_{t_i}$  and  $AL_{t+1}$  makes ARMA models much more accurate than MA filters.

For the first 5,000 points of the database the  $PC$ - $AL$  model with  $m = 2$  reproduces in-sample data with a correlation of 98% and an rms error of  $0.19 \sigma_{AL}$ . The correlation and error change by 0.1% or less when  $m$  is varied between 1 and 6. For  $PC$ - $AU$  the model with  $m = 2$  gives a correlation of 97% and an error of  $0.22 \sigma_{AU}$ .

Eq. (3) can produce out-of-sample, iterated predictions for a test set which is a small subset of the database. We ensure that the predictions are out-of-sample by using database points which are outside the test set and at least 480 steps before or after the set. We iterate the prediction by calculating  $\widehat{AL}_{t+1}$  from (3), at the next step using  $\widehat{AL}_{t+1}$  on the right-hand side of (3) to predict  $\widehat{AL}_{t+2}$ , and so on. After  $m$  steps, all the  $AL_{t-i}$  terms are taken from predictions while the  $PC_{t-i}$  terms in (3) are updated from observations. In this way we make iterated predictions for 100 time steps (4.16 hours). After varying  $m$  in the range 1–6 we find the most accurate predictions for  $m = 2$ , so we fixed  $m$  to that value. For the interval  $(t_0, t_0+100)$  the average prediction error,  $E$ , is:

$$E_{t_0}^2 \equiv \frac{1}{100 \sigma_{AL}^2} \sum_{i=1}^{100} (\widehat{AL}_{t_0+i} - AL_{t_0+i})^2 \quad (4)$$

The error is then averaged over several initial conditions,  $t_0$ .

Fig. 2 shows predictions of ten successive intervals. The top two panels display the observed  $AL/AU$  as a function of time (black line) where the prediction error indicated by the shaded area, while the third panel displays the  $PC$  index input. Low-frequency intensifications are predicted well, but high-resolution events such as substorm onsets and are not reproduced systematically.

We average the time sequence of the  $AU$  prediction error over 100 intervals (upper part of Fig. 3). It increases for about an hour until it reaches the asymptotic value of 20 nT. The asymptotic error for  $AL$  is 40 nT (lower part of Fig. 3, where we have multiplied the  $AL$  error with  $-1$ ). The asymptotic error is small, so long-term predictions are quite accurate on the average.

More importantly, the asymptotic prediction error for  $AU$  ( $AL$ ) is 40% (25%) lower than the prediction error obtained from ISEE 3 solar wind data, shown as the dotted lines in Fig. 3. (The ISEE 3 data were propagated ballistically to a nominal subsolar magnetopause, and the distribution of the prediction error is very similar to the distribution of error from predictions based on near-Earth IMP-8 solar wind data.) Thus the  $PC$  index is a much more accurate precursor than solar wind input. The two are complementary: the solar wind has a significant lead time (0.5–1 hour for propagation to magnetopause plus 20 min for intensification of convection electrojets) and can be used for forecasting, while the  $PC$  index lead time is short (7.5–17.5 min; Fig. 1) and only advantageous for specification (“nowcasting”).

Finally, the asymptotic error of  $PC$ -based predictions is small compared to the standard deviations of the indices ( $\sigma_{AU} = 60$  nT,  $\sigma_{AL} = 164$  nT for the whole dataset). This confirms first that polar cap and auroral zone geomagnetic disturbances are induced by a common source, i.e. field-aligned currents. Second, this is an example of coherent magnetospheric activity in two different coupled regions: electrody-

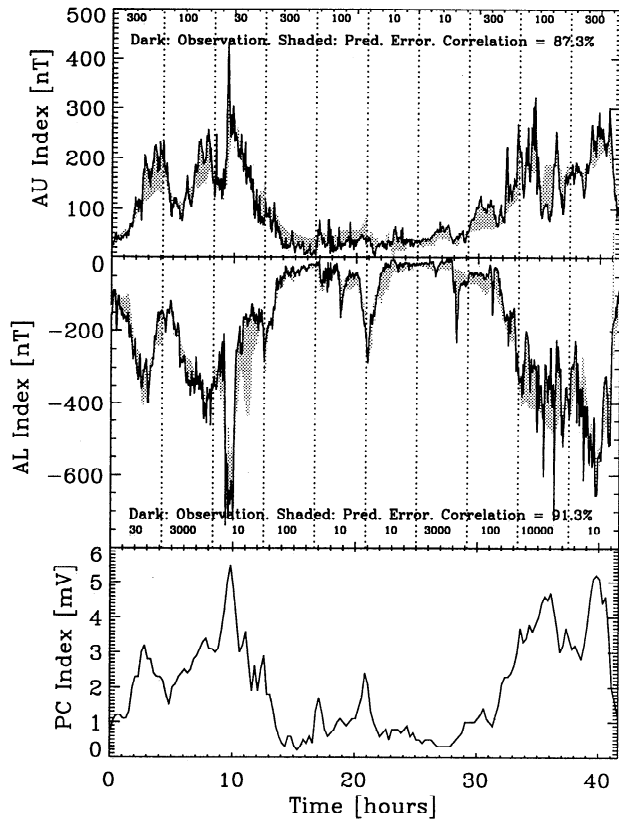


Figure 2. Prediction of  $AL$  and  $AU$  indices (top two panels) from the  $PC$  index (third panel). The dark curves show observations while the shading indicates the prediction error. We separately predict ten successive intervals of  $AL/AU$  of 100 steps (4.16 hours); they are demarcated by the vertical dotted lines. The correlation figures have been computed over all ten intervals.

dynamic coupling of the polar cap and auroral zone allows for accurate specification of variables of one region from variables of the other.

## Nonlinear ARMA Models

Although linear models are quite accurate in reproducing  $AL/AU$  indices, the physical relation between the underlying processes may be nonlinear, either because of the physics or the measurement process, and then nonlinear models may improve the prediction accuracy significantly by capturing features inaccessible to linear methods.

In the nonlinear ARMA model

$$\tilde{A}L_{t+1} = \sum_{i=0}^{m-1} \tilde{A}_i AL_{t-i} + \sum_{i=0}^{m-1} \tilde{B}_i PC_{t-i} \quad (5)$$

the coefficients  $\tilde{A}_i$ ,  $\tilde{B}_i$  are now functions of  $\mathbf{AL}_t \equiv (AL_t, AL_{t-1}, AL_{t-2}, \dots)$ , and  $\mathbf{PC}_t \equiv (PC_t, PC_{t-1}, PC_{t-2}, \dots)$ . The vector  $(\mathbf{AL}_t, \mathbf{PC}_t)$  is the initial condition. Whereas in the linear model (3) the coefficients were calculated from 5,000 points, a number comparable to the size of the database, we calculate the coefficients of (5) from much smaller sets of  $NN$  points,  $t' = 1, 2, \dots, NN$ , for which the Euclidean distance from the initial condition  $[(\mathbf{AL}_{t'}, \mathbf{PC}_{t'}) - (\mathbf{AL}_t, \mathbf{PC}_t)]$  is minimum [see also: Vassil-

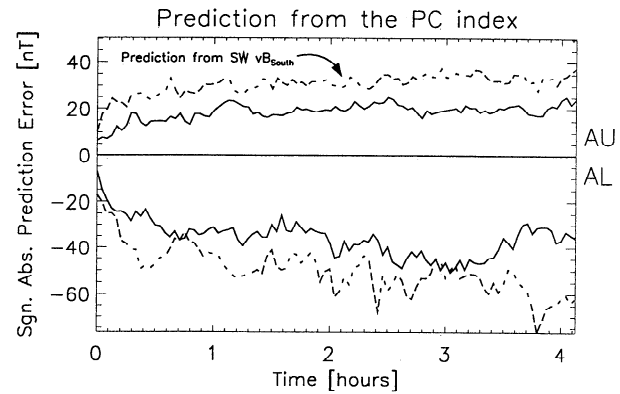


Figure 3. Prediction errors of  $AU$  (upper two curves) and  $AL$  as a function of time. The prediction errors for  $AL$  have been multiplied by  $-1$ . Predictions based on the  $PC$  index as input (solid lines) are at least 30% more accurate than predictions based on ISEE-3-measured, propagated solar wind input (dotted lines). Each curve is averaged over 50 intervals.

iadis et al., 1995]. These are the nearest neighbors of the initial condition. Note that because the indices have very different range values, we normalize each one so that its distribution has unit standard deviation. The prediction error is again given by Eq. (4) while the smallest error as a function of  $NN$  is denoted by  $E_{min}$  and the minimizing  $NN$  by  $NN_{opt}$ .

The  $PC$ - $AL$  relation is represented by a nonlinear model if (a) the optimal number  $NN_{opt}$  is much smaller than the linear limit  $NN_{max} = N - m$ ; and (b) the nonlinear prediction is significantly more accurate than the linear ARMA prediction,  $E_{min} \ll E_{lin}$ .

We compare the linear and nonlinear models using 3-step, or 7.5-min, predictions over the first two days in November 1978. (The prediction interval should be small compared to the time it takes for the error to saturate, 1 hour as shown in Fig. 3.) The number  $NN$  is varied in a range from the smallest value,  $2m$ , to the largest possible,  $N - m = 69118$ . For criterion (a) above we find that generally the optimal value,  $NN_{opt}$ , is a small number (10–100) compared to  $N - m$  (Fig. 4) so the most accurate predictions are made by nonlinear models most of the time. The nonlinear model is more accurate also for 12-step and 100-step predictions. For criterion (b) the best nonlinear prediction is also more accurate than the linear prediction, however the difference is not large. The average best-prediction errors for  $AL$  is  $E = 0.12$ , or 60% of the average linear-prediction error (0.19). The two error distributions are shown for  $AL$  (Fig. 5a) and  $AU$  (Fig. 5b). For 12-step and 100-step predictions the linear and nonlinear prediction errors are much more similar and for even longer prediction times they converge to a common asymptotic error value, that of Fig. 3. Thus the relation between the  $PC$  index and either electrojet index is best modeled by a nonlinear model, but the average effect of the nonlinearity on prediction error is small.

## Concluding Remarks

We examined the  $PC$  index as an input to electrojet index models considering them as three independent magnetospheric variables. Phase differences of the order of 7.5 and 17.5 min between the indices are explained by the auroral

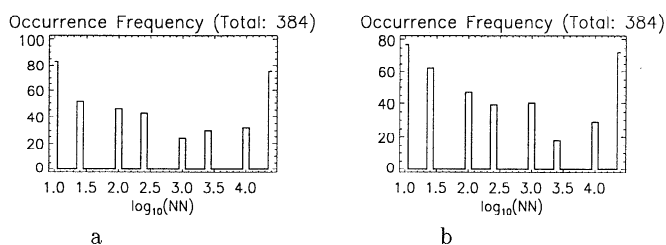


Figure 4. (a) The nonlinearity in the *PC-AL* relation is measured by the number of nearest neighbors necessary to make the most accurate prediction. The number,  $NN_{opt}$ , is distributed between small values (high nonlinearity) and large (low nonlinearity) compared to the database size,  $N = 69,120$  (linearity). The frequency of occurrence is shown as a histogram of 384 values. Each value corresponds to 7.5 min intervals. Most of the  $NN_{opt}$  are small indicating nonlinearity. (b) Same for *PC-AU*.

oval equatorward expansion over the AE-measuring stations. The relative phase and the activity level appeared uncorrelated. We constructed several types of empirical models and found significantly higher correlations (up to 97–98% for linear ARMA models) than any previous studies. The best model for the relation between *PC* and *AL/AU* was nonlinear, i.e. it depended systematically on the activity level; however it is a relatively small improvement over the linear model as far as prediction error is concerned.

The high correlation between geomagnetic activity from the polar cap and auroral zone shows that the two regions are strongly coupled. The electromagnetic coupling allows the two magnetospheric regions to produce coordinated, organized activity [Baker et al., 1990; Klimas et al., 1996]. In practical terms, because of the coupling one region's measurements can be used to accurately estimate activity of the other, which is significant for nowcasting and forecasting purposes. Currently a preliminary *PC* index is issued every day from the Danish Meteorological Institute and we are using nonlinear models on these data to specify and predict *AL* and *AU*. There are plans to supply the *PC* index in near-real time (S. Vennerstroem, 1995, priv. comm.). The *PC* index is expected to rapidly become important for specification of the magnetospheric state, and useful in scientific and space weather applications.

**Acknowledgments.** We thank E. Erwin (NGDC), and E. Friis-Christensen and S. Vennerstroem (DMI) for providing the *PC* index data; and C. Russell and M. Kniffin (UCLA) for providing the ISEE 3 data. D. Vassiliadis thanks O. Troshichev, V. Papitashvili and N. Maynard for useful discussions.

## References

- Akasofu, S.-I., B.-H. Ahn, Y. Kamide, and J. H. Allen, A note on the accuracy of the auroral electrojet indices, *J. Geophys. Res.*, **88**(A7), 5769–5772, 1983.
- Baker, D. N., A. J. Klimas, R. L. McPherron, and J. Büchner, The evolution from weak to strong geomagnetic activity: An interpretation in terms of deterministic chaos, *Geophys. Res. Lett.*, **17**, 41, 1990.
- Baumjohann, W., Merits and limitations of the use of geomagnetic indices in solar wind-magnetosphere coupling studies, in *Solar Wind-Magnetosphere Coupling*, Kamide, Y., and J. A. Slavin, editors, p. 3–15, Tokyo, Terra Scientific, 1986.

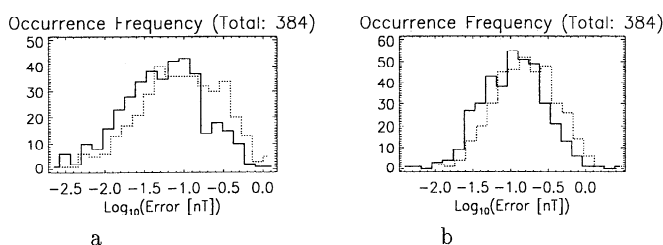


Figure 5. (a) Occurrence frequency of prediction errors of the 384 7.5-min *AL* predictions of Fig. 5a. The solid-line histogram is for the best predictions (whether linear or nonlinear). The dashed-line histogram shows the linear-prediction errors. The average best prediction is 40% more accurate than the average linear one. (b) Same for *PC-AU*.

- Holzer, R. E., and J. A. Slavin, Processes influencing the diurnal variation of the *AL* index and its reliability, *J. Geophys. Res.*, **86**(A11), 8977–8980, 1981.
- Klimas, A. J., D. Vassiliadis, D. N. Baker, and D. A. Roberts, The organized nonlinear dynamics of the magnetosphere, *J. Geophys. Res.*, **101**(A6), 13089, 1996.
- Kroehl, H. W., A critical evaluation of the AE indices, *J. Geomag. Geoelectr.*, **41**, 317–329, 1989.
- Mayaud, P. N., *Derivation, Meaning and Use of Geomagnetic Indices*, AGU, Washington, DC, 1980.
- Rostoker, G., and T. D. Phan, Variation of auroral electrojet spatial location as a function of the level of magnetospheric activity, *G. Geophys. Res.*, **91**(A2), 1716–1722, 1986.
- Troshichev, O. A., V. G. Andrezen, S. Vennerstroem, and E. Friis-Christensen, Magnetic activity in the polar cap - a new index, *Planet. Space Sci.*, **33**, 275, 1988.
- Troshichev, O. A., The physics and meaning of the existing and proposed high-latitude geomagnetic indices, *Annales Geophysicae*, **6**(6), 601–610, 1988.
- Vassiliadis, D., A. J. Klimas, D. N. Baker, and D. A. Roberts, A description of solar wind-magnetosphere coupling based on nonlinear filters, *J. Geophys. Res.*, **100**(A3), 3495, 1995.
- Vennerstroem, S., E. Friis-Christensen, O. A. Troshichev, and V. G. Andrezen, Comparison between the polar cap, *PC*, and the auroral electrojet indices *AE*, *AL*, and *AU*, *J. Geophys. Res.*, **96**(A1), 101–113, 1991.

V. Angelopoulos, Space Sciences Laboratory, University of California, Berkeley, CA 94720-7450. (e-mail: vassilis@ssl.berkeley.edu)

D. N. Baker, Laboratory for Astrophysics and Space Physics, 1234 Innovation Dr., University of Colorado, Boulder, CO 80309. (e-mail: baker@lynx.colorado.edu)

A. J. Klimas and D. Vassiliadis, Laboratory for Extraterrestrial Physics, Code 692, NASA Goddard Space Flight Center, Greenbelt, MD 20771. (e-mail: u2ajk@lepajk.gsfc.nasa.gov; vassi@lepgst.gsfc.nasa.gov)

(Received: December 21, 1995; revised: March 29, 1996; accepted: June 12, 1996)